Electronic Supplementary Material (ESI) for Physical Chemistry Chemical Physics.

Boosting water oxidation activity by tuning the proton transfer process of cobalt phosphonates in neutral solution

Jiangquan Lv,* Xiangfeng Guan, Muxin Yu, Xiaoyan Li, Yunlong Yu, and Dagui Chen

Corresponding E-mail: jqlv@fjjxu.edu.cn

Supplementary Figures.

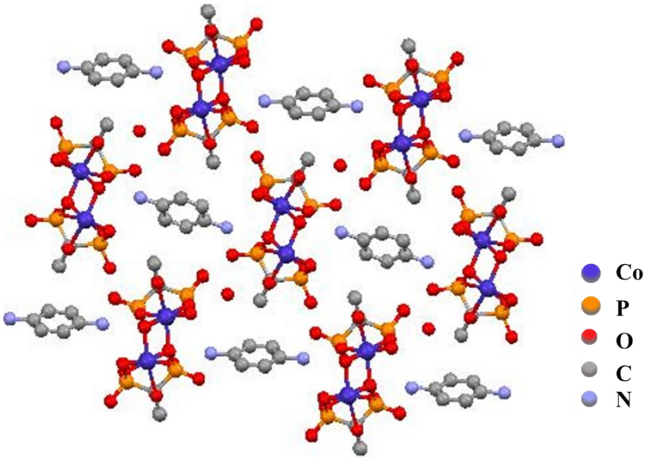

Figure S1. The three-dimensional supramolecular network structure of Co-PDA.

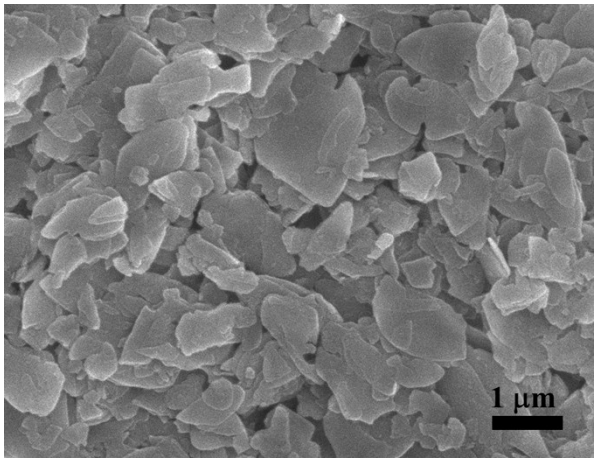

Figure S2. The SEM image of the Co-NH_4^+.

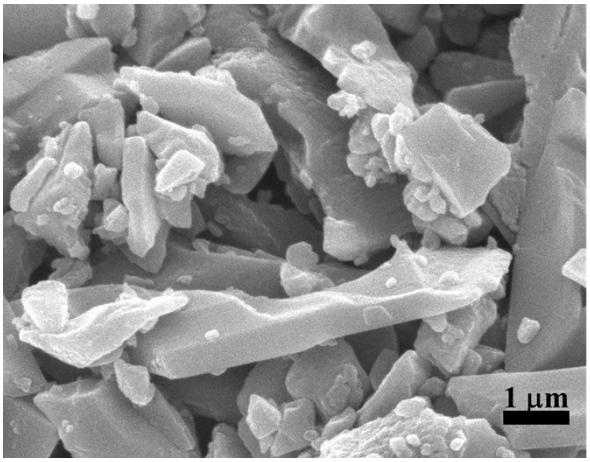

Figure S3. The SEM image of the Co-PDA.

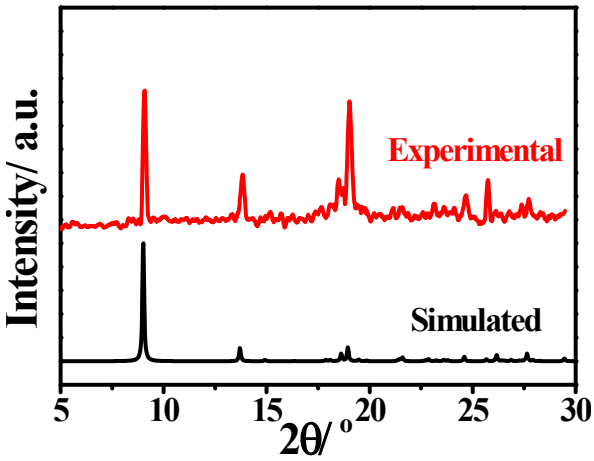

Figure S4. The XRD pattern and the simulated result of Co-NH_4^+.

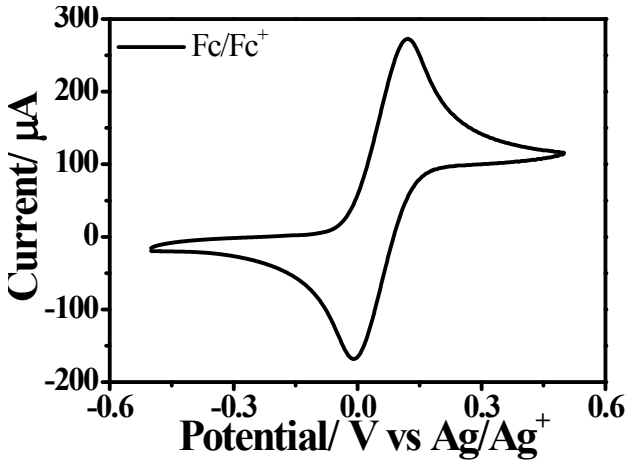

Figure S5. CV of ferrocene/ferrocenium (Fc/Fc^+) using Ag/Ag^+ (1M) reference electrode.

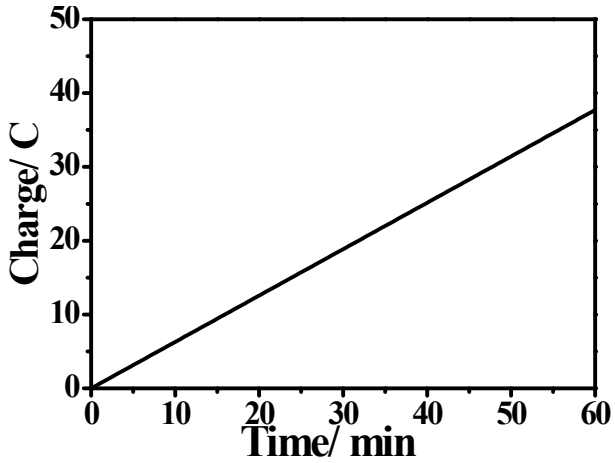

Figure S6. Controlled potential electrolysis of Co-PDA at 1.4 V vs Fc/Fc^+ resulting 94% Faradaic efficiency for O_2 evolution.

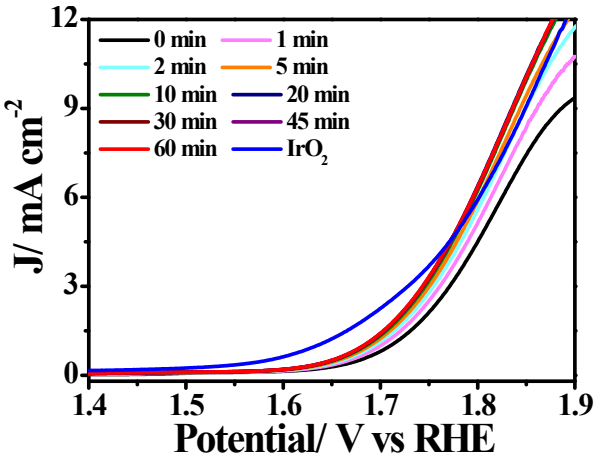

Figure S7. LSV curves of Co-PDA which was immersed in 50 mM PBS solution for periods of time before tests.

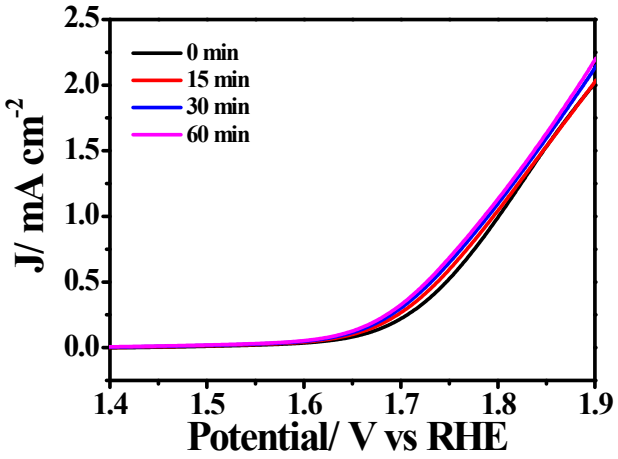

Figure S8. LSV curves of Co-NH_4^+ which was immersed in 50 mM PBS solution for periods of time before tests.

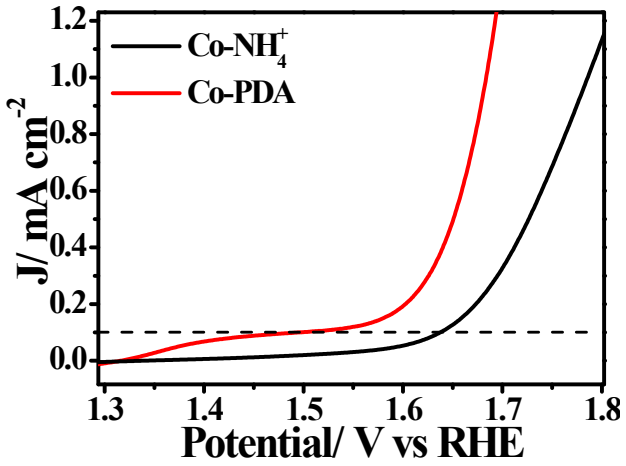

Figure S9. The enlarged part of LSV of Co-PDA and Co-NH_4^+ to better show the onset potential.

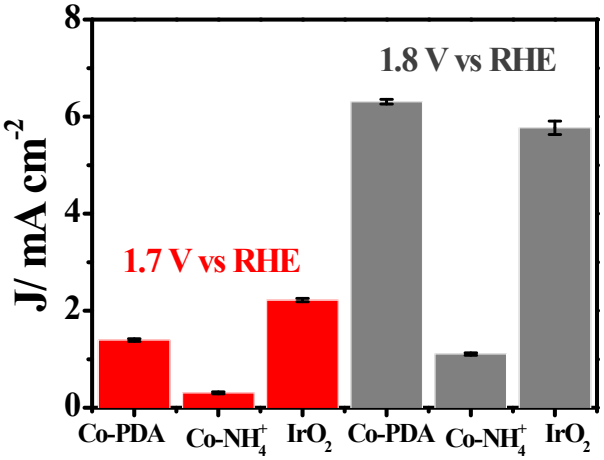

Figure S10. The OER performance of Co-PDA, Co-NH_4^+ and IrO_2 at different potential with errors bars to better show the reproducibility.

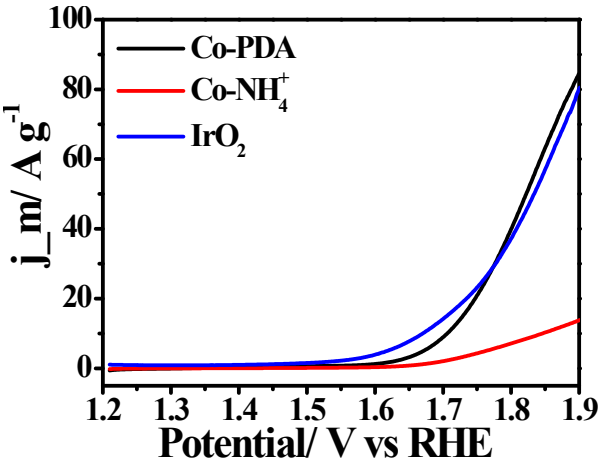

Figure S11. The mass current density j_m vs potential curves of Co-PDA, Co-NH_4^+ and IrO_2.

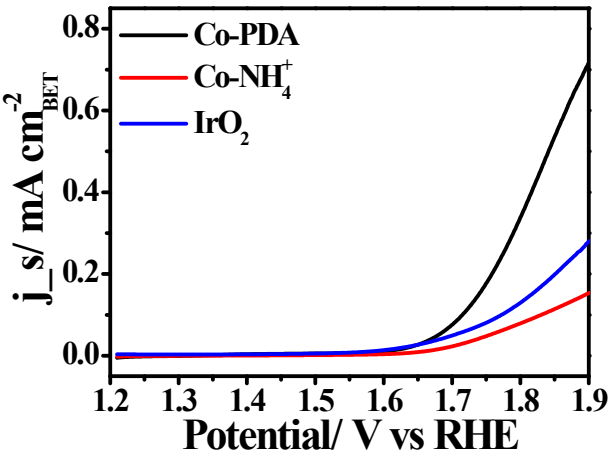

Figure S12. The specific current density j_s vs potential curves of Co-PDA, Co-NH_4^+ and IrO_2.

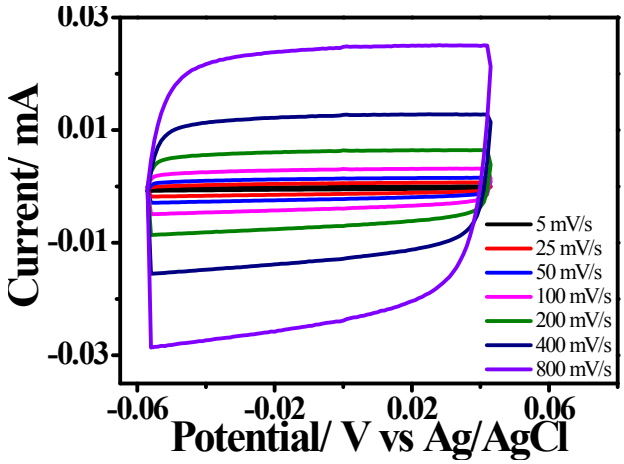

Figure S13. CV curves of Co-PDA were measured in a non-Faradaic region at the following scan rate: 5, 10, 25, 50, 100, 200, 400, and 800 mV s^{-1}.

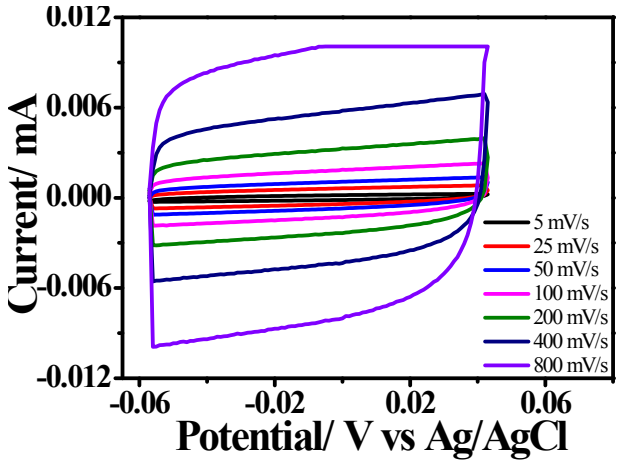

Figure S14. CV curves of Co-NH_4^+ were measured in a non-Faradaic region at the following scan rate: 5, 10, 25, 50, 100, 200, 400, and 800 mV s^{-1}.

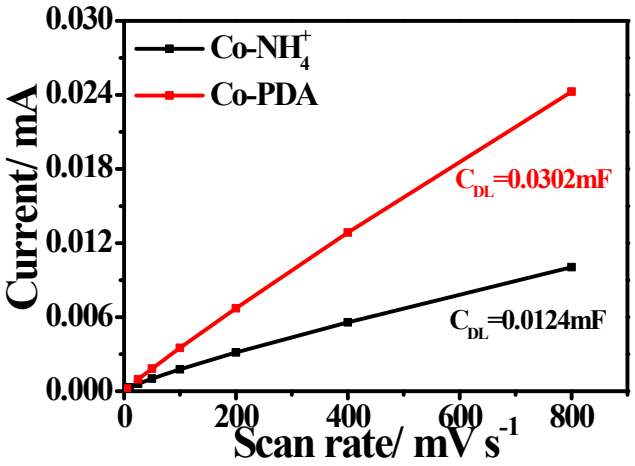

Figure S15. Double-layer capacitance (C_d) datas derived from CV measurements at different scan rate for Co-PDA and Co-NH_4^+.

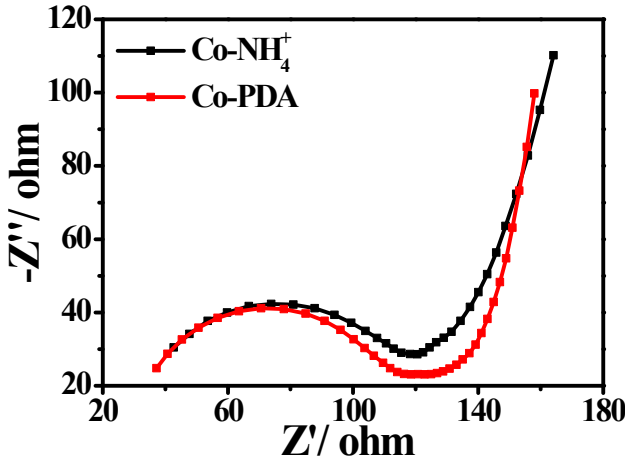

Figure S16. The electrochemical impedance spectra (EIS) of Co-PDA and Co-NH_4^+.

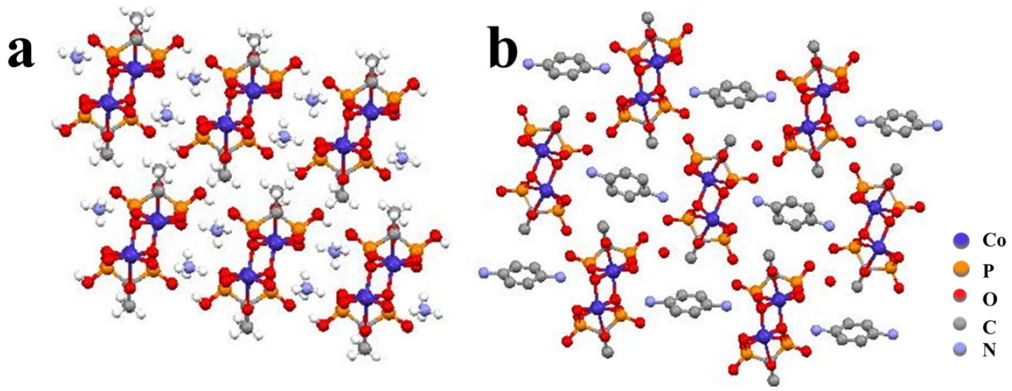

Figure S17. The three-dimensional supramolecular network structure of Co-PDA and Co-NH_4^+ showed the same $Co_2(hedpH)_2^{2-}$ core structure.

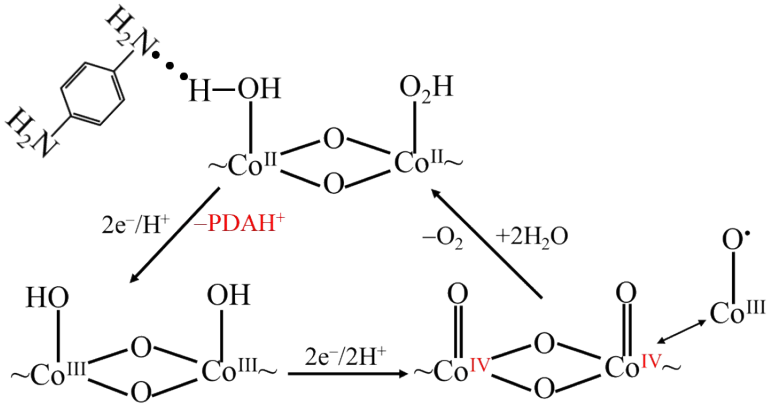

Figure S18. Possible water oxidation pathway for Co-PDA.

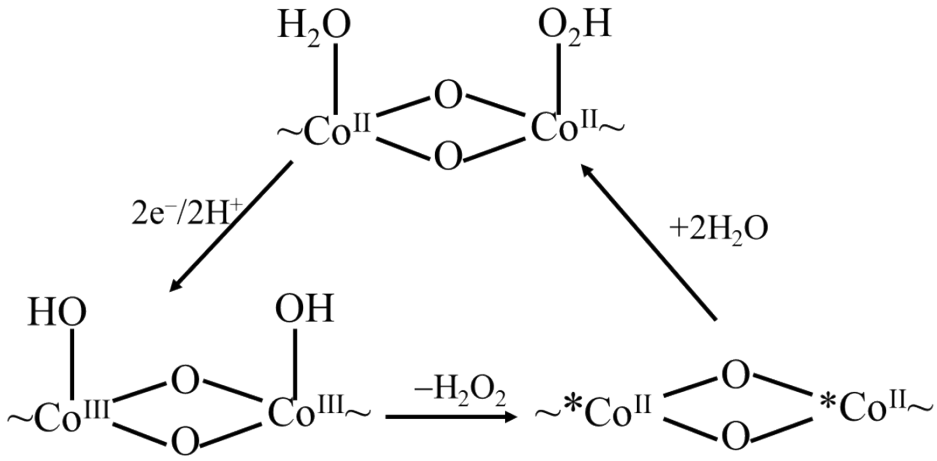

Figure S19. Possible water oxidation pathway for Co-NH_4^+.

Supplementary Table.

Table S1. Comparison of the OER performance in neutral condition (pH=7).

Substrate	Catalyst	η_{onset} (mV)	Tafel slop (mV/dec)	Reference
Glassy carbon	Co-PDA	250	119	This work
Glassy carbon	Co-NH_4^+	410	303	This work
Ti mesh	Co-Pi	180	187	S1
Glassy carbon	Cobalt(II) phosphonates	484	83	S2
Carbon cloth	Co-Pi	340	60	S3
Glassy carbon	MAF-69-Mo	270	144	S4
Carbon fiber paper	$Ni_{0.1}Co_{0.9}P$ nanosheets	250	148	S5

Table S2. The summary of BET surface areas of Co-PDA, Co-NH_4^+ and IrO_2.

Sample name	BET surface areas (m^2/g)
Co-PDA	11.8
Co-NH_4^+	8.99
IrO_2	28.7

Supplementary References

S1. L. Xie, R. Zhang, L. Cui, D. Liu, S. Hao, Y. Ma, G. Du, A. M. Asiri and X. Sun, *Angewandte Chemie International Edition*, 2017, **56**, 1064-1068.

S2. T. Zhou, D. Wang, S. Chun-Kiat Goh, J. Hong, J. Han, J. Mao and R. Xu, *Energy Environ. Sci.*, 2015, **8**, 526-534.

S3. A. Irshad and N. Munichandraiah, *ACS Applied Materials & Interfaces*, 2015, **7**, 15765-15776.

S4. Y.-T. Xu, Z.-M. Ye, J.-W. Ye, L.-M. Cao, R.-K. Huang, J.-X. Wu, D.-D. Zhou, X.-F. Zhang, C.-T. He, J.-P. Zhang and X.-M. Chen, *Angewandte Chemie International Edition*, 2019, **58**, 139-143.

S5. R. Wu, B. Xiao, Q. Gao, Y.-R. Zheng, X.-S. Zheng, J.-F. Zhu, M.-R. Gao and S.-H. Yu, *Angewandte Chemie International Edition*, 2018, **57**, 15445-15449.